Review

Nanomaterial-based advanced oxidation/reduction processes for the degradation of PFAS

Inês M. F. Cardoso, Luís Pinto da Silva and Joaquim C. G. Esteves da Silva *

Chemistry Research Unit (CIQUP), Institute of Molecular Sciences (IMS), Department of Geosciences, Environment and Territorial Planning, Faculty of Sciences, University of Porto (FCUP), Rua do Campo Alegre s/n, 4169-007 Porto, Portugal; up201704720@edu.fc.up.pt (I.M.F.C.); luis.silva@fc.up.pt (L.P.d.S.)

* Correspondence: jcsilva@fc.up.pt (J.E.S.); Tel.: +351-220-402-569

Abstract: This review focus on a critical analysis of nanocatalysts for Advanced Reductive Processes (ARP) and Oxidation Processes (AOP) designed for the degradation of poly/perfluoroalkyl substances (PFAS) in water. Ozone, ultraviolet and photocatalyzed ARP and/or AOP will be the basic treatment technologies. Besides the review of the nanomaterials with greater potential as catalyst for advanced processes of PFAS in water, the perspectives for its future development considering sustainability considerations will be discussed. Moreover, a brief analysis of the current state of the art of the ARP and AOP for the treatment of PFAS in water will be presented.

Keywords: Poly/perfluoroalkyl substances; advanced reductive processes; advanced oxidation processes; nanomaterials; water treatment.

1. Introduction

Poly- and perfluoroalkyl substances (PFAS) are a huge class of mainly fluorinated anionic surfactants, consisting of a hydrophobic carbon-fluorine straight or branched chain and a hydrophilic functional group, with over 3000 compounds that have been made and used since the 1950s [1]. PFAS can be classified under three subclasses [2]: perfluoroalkyl sulphonoic acids (PFSA); perfluoroalkyl carboxylic acids (PFCA); fluorotelomer-based substances (precursor compounds). The two most representative PFAS are the PFCA perfluorooctanoic acid (PFOA) and the PFSA perfluorooctane sulfonate (PFOS), because they were extensively produced and studied [3]. Due to their persistence, bioaccumulation, and toxicity, some of these substances are now listed in the Stockholm Convention as new POPs [4]. Human exposition to these substances occurs mainly through food ingestion and drinking water [3]. PFAS have been detected in wastewaters of municipal wastewater treatment plants without known direct industrial sources [5].

Currently, due to a myriad of applications [1-7], PFAS are ubiquitous in environmental water, and sustainable remediation strategies must be designed to improve the quality of water and reduce human health risks burdens. However, due to the high chemical strength of the carbon to fluorine bond, PFAS are known to be highly recalcitrant to conventional water treatment processes [2,6,7]. Due to this limitation, adsorption, membranes and ion-exchange technologies, which are efficient in their capture from water sources, are being proposed [8-12]. However, these technologies do not destroy PFAS and produce solid-wastes that require incineration, which raises serious sustainability questions [6]. High energy technologies, like plasma, electron beams and gamma rays, have been successful in the destruction of PFAS, but their practical use is limited [2,6]. Also, some mechanochemical, electrochemical and sonochemical methodologies showed potential, but major up-scaling challenges limit they utilization [2,6].

Advanced reduction and oxidation processes (ARP and AOP) using ozone, persulfate, hydrogen peroxide and ultraviolet can be easily implemented in water treatment stations, and have shown promising results in the degradation of PFAS [13-16]. Persul-

Preprints (www.preprints.org) | NOT PEER-REVIEWED | Posted: 25 April 2023 doi:10.20944/preprints202304.0927.v1

fate-based AOP, that generate sulphate radical, seems to be a better oxidant of PFAS [13,16]. Photochemical heterogeneous catalytic AOP have shown to degrade efficiently PFAS [5-7,17,18].

Nanomaterial-based treatment technologies for PFAS in water have been proposed taking into consideration their high surface specific area (SSA), which would have improved the adsorption capabilities, and their designed increased reactivity, particularly as photocatalysts [19-23]. Titanium and Indium oxides have been shown to be particularly active in the catalysis of photochemical decomposition of PFAS [19,21,22]. Carbon-based nanomaterials, namely carbon nanotubes and graphene and its derivatives, have also been proposed for the degradation of PFAS, taking into consideration their high hydrophobicity, which is particularly adjustable for the adsorption of the hydrophobic carbon-fluorine chain of PFAS [23].

The objective of this review is to present, and critically discuss, the currently standard ARP and AOP that can be used for PFAS degradation in water, and to review the nanomaterials that are currently being proposed to be coupled to advanced processes for water PFAS treatment. In the case of the nanomaterials this review will focus mainly on the publications and research trends in the last two years.

2. Advanced oxidation/reduction processes

AOP and ARP combine activation methods and chemical agents to form reactive radicals that will degrade PFAS compounds. The degradation efficiency can be measured using different indicators, like the "F index", overall defluorination ratio (overall deF%) and molecular defluorination ratio (molecular deF%):

$$\text{F index} = [F^-]_{released} / [PFAS]_{degraded} \quad (1)$$

$$\text{Overall deF\%} = 100 \times [F^-]_{released} / \{[PFAS]_0 \times N_{C\text{-}F}\} \quad (2)$$

$$\text{Molecular deF\%} = 100 \times [F^-]_{released} / \{[PFAS]_{degraded} \times N_{C\text{-}F}\} \quad (3)$$

where, $[F^-]_{released}$ is the molar concentration of fluoride released; $[PFAS]_0$ is the initial molar concentration of PFAS; $[F^-]_{degraded}$ is the molar concentration of PFAS degraded; and $N_{C\text{-}F}$ is the number of C-F chemical bounds in the parent PFAS molecule.

2.1. ARP

The molecular degradation processes in ARP typically involve the hydrated electron (e_{aq}^-), hydrogen atoms (H^*), and others, due to the specific chemical that is used, like for example when coupled with sulfite anions, the sulfite radical anions (SO_3^{*-}) are also produced [27,36].

2.2.1. Ultraviolet light (254 nm) systems

The photoionization of sulfite in water under standard UV light (254 nm) (UV systems) is described by the following chemical equation:

$$SO_3^{2-} + h\nu \rightarrow SO_3^{*-} + e_{aq}^- \quad (4)$$

The reactivity of the hydrated electron is capable to break the carbon fluorine chemical bond of the PFAS and in a treatment process its concentration must be maximized. The pH will be an important factor in the hydrated electron speciation because it reacts with protons, accordingly to the following equation:

Preprints (www.preprints.org) | NOT PEER-REVIEWED | Posted: 25 April 2023 doi:10.20944/preprints202304.0927.v1

$$e_{aq}^- + H^+ \rightarrow H^* \quad (5)$$

However, if alkaline pH is used (for example, pH=10-12), the hydrated electron is regenerated according to the following equation [37,38]:

$$H^* + OH^- \rightarrow H_2O + e_{aq}^- \quad (6)$$

Therefore, alkaline conditions are preferred for the degradation of PFAS in water. The presence of the anions nitrate and carbonate will quench the hydrated electron inhibiting its degradation efficiency [38]. Also, increasing the temperature and the solute dose will increase the degradation and defluorination efficiencies - in the case of the solute dose, a critical value is observed above which no increase occurs [27].

The degradation mechanism of the PFOA molecules by the hydrated electron follows by H/F exchange and chain shortening (Figure 1) [27]. In the case of PFOS, besides similar H/F exchange and chain shortening via C-C cleavage, a desulfonation mechanism is observed (Figure 2) [27].

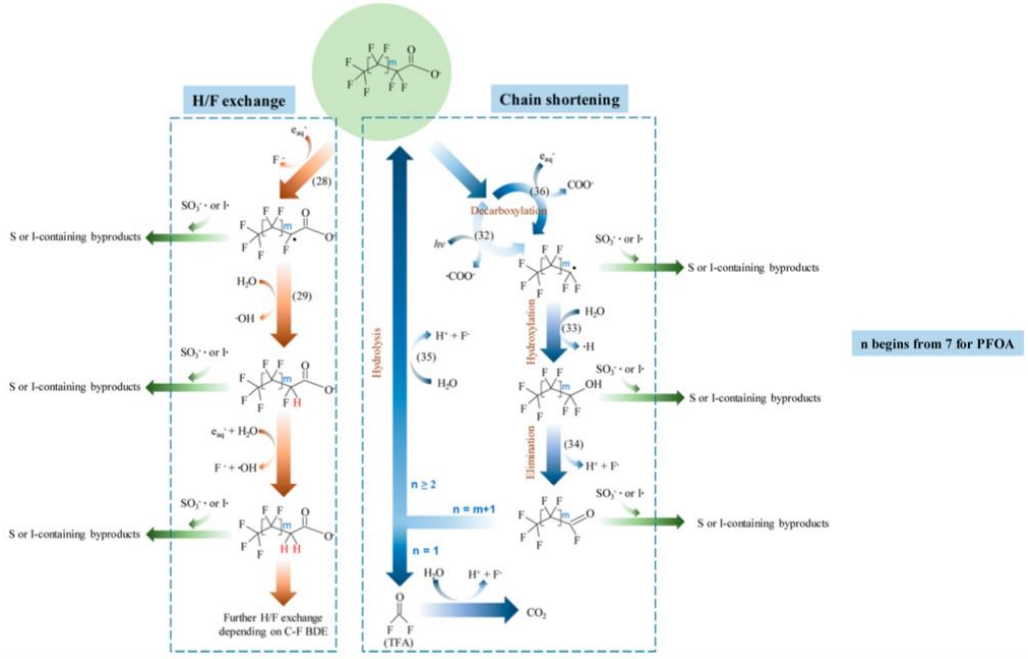

Figure 1. Proposed major pathways of reductive degradation of PFOA. Adapted with permission from reference [27]. Copyright {2020} American Chemical Society.

Preprints (www.preprints.org) | NOT PEER-REVIEWED | Posted: 25 April 2023 doi:10.20944/preprints202304.0927.v1

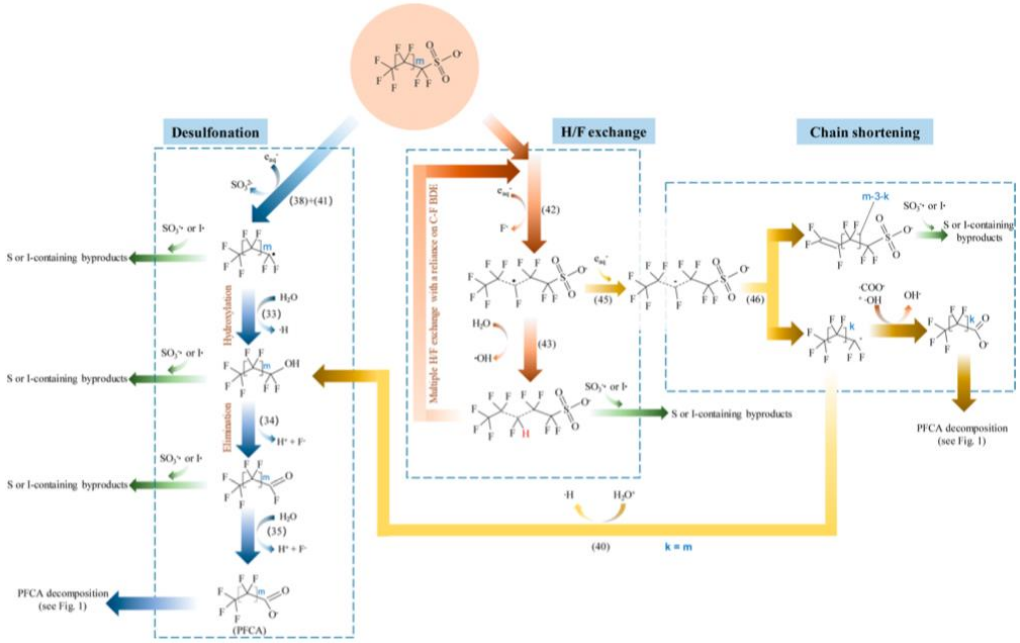

Figure 2. Proposed major pathways of reductive degradation of PFOS. Adapted with permission from reference [27]. Copyright {2020} American Chemical Society.

2.2.2. Vacuum ultraviolet light (185 nm) systems

Contrary to the common UV systems, the vacuum ultraviolet light systems (VUV), emitting in the high-energy wavelength region (185 nm/647 kJ/mol), can directly decompose PFAS molecules [39,40]. Moreover, these systems can produce more hydrated electrons due to the water photolysis (*OH - hydroxyl radical):

$$H_2O + h\nu \rightarrow H^{*} + {}^{*}OH \quad (7)$$

$$H_2O + h\nu \rightarrow H^{+} + e_{aq}^{-} + {}^{*}OH \quad (8)$$

In order to improve the hydrated electron production, VUV is coupled to the chemical agents iron(III) in acid aqueous solution [39] and sulfite in neutral to alkaline aqueous solutions [40]. In these cases, equation (4) is also observed and, when iron(III) is present, the formation of complexes between ferric ions and PFOA improves the degradation efficiency [39].

When ferric ion is used in the VUV, the defluorination rates increased 2.6 times [39] and, when sulfide is present, the PFOS decomposition rate increased nearly 7.5 and 2 folds faster than that in sole VUV and UV/sulfite systems, respectively [40].

In the case of the VUV/sulfite, the degradation mechanism depends on the pH of the solution: at pH=6 the direct photolysis of PFOS is observed; and, in alkaline condition (pH>9), the decomposition occurs via hydrated electron induction [40].

2.2. AOP

Different activation methods are commonly used in AOP that can easily be scaled up in real water or wastewater treatment stations, and, in this review, we will focus on ozone, UV and heterogeneous photocatalysis.

The molecular degradation processes in AOP are designed for the production of the hydroxyl radical (*OH), or other reactive oxygen species (ROS) that can be transformed into the hydroxyl radical, like the superoxide (O_2^{*-}) and peroxyl (HO_2^{*}) radicals. *OH radicals are extremely reactive oxidizers (oxidation potential of the OH radical is ap-

Preprints (www.preprints.org) | NOT PEER-REVIEWED | Posted: 25 April 2023 doi:10.20944/preprints202304.0927.v1

proximately 2.8 V) and non-selective towards organic pollutants in water [41-43]. Other specific strong oxidant radical species can be produced when other chemical precursors are coupled with basic AOP, like for example persulfate anion that generates the sulfate radical (SO_4^{*-}) [43].

The degradation of PFAS by the hydroxyl radical was referred as a minor pathway, which was justified by use of experimental conditions where the production yield of this radical was low [44-47]. However, other different experimental conditions of the AOP resulted in quantitative degradation efficiencies which makes ozone, and particularly when coupled with other agents, useful AOP for the degradation of PFAS. Some of the observed low efficiencies of AOP in the PFAS degradation, is related to the high reduction potential of fluorine (E^o = 3,6 V), which makes the oxidation of fluoride to elemental fluorine thermodynamically unfavorable [46].

2.2.1. Ozone

Bubbling ozone gas in water generates a mixture of unstable reactive species where hydroxyl radical is the major secondary oxidant [41,42]. The decomposition of ozone initiates with the reaction with hydroxide ions, involving reactions (9) to (11); depending on the pH of the aqueous solution, it evolves according to the different mechanisms depicted in reactions (12) to (16) [42].

$O_3 + OH^- \rightarrow HO_2^- + O_2$ (9)
$O_3 + HO_2^- \rightarrow {}^*OH + O_2^{*-} + O_2$ (10)
$O_3 + O_2^{*-} \rightarrow O_3^{*-} + O_2$ (11)

pH <≈ 8
$O_3^{*-} + H^+ \rightleftharpoons HO_3^*$ (12)
$HO_3^{*-} \rightarrow {}^*OH + O_2$ (13)

pH >≈ 8
$O_3^{*-} \rightleftharpoons O^{*-} + O_2$ (14)
$O^{*-} + H_2O \rightarrow {}^*OH + OH^-$ (15)
${}^*OH + O_3 \rightarrow HO_2^* + O_2$ (16)

To increase hydroxyl radical production, ozone can be coupled to hydrogen peroxide (H_2O_2) in the so-called peroxone process [48,49]. The hydroxyl radical production mechanism in the peroxone process is [49]:

$H_2O_2 \rightleftharpoons HO_2^- + H^+$ (17)
$HO_2^- + O_3 \rightarrow HO_2^* + O_3^{*-}$ (18)
$O_3^{*-} + H^+ \rightarrow HO_3^{*-}$ (19)
$HO_3^{*-} \rightarrow O_2 + OH^*$ (20)
$OH^* + H_2O_2 \rightarrow HO_2^* + H_2O$ (21)

The analysis of equation (21) shows that the relative amount of hydrogen peroxide can provoke the quenching of the hydroxyl radical. Consequently, there exists an optimum ratio between ozone/hydrogen peroxide that maximizes the production of hydroxyl radical and the efficiency of the peroxone process [49].

Ozone can be coupled with 254 nm UV light (Ozone/UV process), which will generate further hydroxyl radical mainly according to the following chemical equations [49]:

$O_3 + h\nu \rightarrow O_2 + O^*$ (22)
$O^* + H_2O \rightarrow 2\ {}^*OH$ (23)

Preprints (www.preprints.org) | NOT PEER-REVIEWED | Posted: 25 April 2023 doi:10.20944/preprints202304.0927.v1

The catalytic degradation of ozone can also promote the formation of hydroxyl radicals enhancing the degradation efficiency of organic molecules. For example, the presence of iron(II) may result in the following chemical equations [50]:

$$Fe^{2+} + O_3 \rightarrow FeO^{2+} + O_2 \quad (24)$$
$$FeO^{2+} + H_2O \rightarrow Fe^{3+} + {}^{*}OH + OH^{-} \quad (25)$$

Molecular ozone has a redox potential of E^{o}=2.07 V and ${}^{*}OH$ an E^{o}=2,8 V, and these characteristics are insufficient for the quantitative degradation of PFAS [46]. The degradation of PFSA and PFCA using 0.300 g of ozone per hour achieved about 22% degradation [46]. However, in another work, PFAS molecules were quantitatively degraded with ozone air fractionation [47]. Also, the degradation of PFOA and PFOS achieved 85 up to 100% via ozonation (2.5 wt% O_3 generated at 85 W at 8.7 g of ozone per hour) under alkaline conditions (pH=11) [44]. Contrary to these last studies, PFOA was only 0.5% defluorinated in 4 hours reaction time using ozone at 0.025 g per hour [14]. The analysis of these results with PFAS and ozone, apparently shows that the higher the ozone dosage is, the higher the degradation efficiency and, also, alkaline pH values increase the degradation efficiency. Nevertheless, apparently the optimum ozone concentration has a threshold due to a self-quenching of the hydroxyl radical [51]. But, the effect of the hydroxyl radical in the PFAS degradation is controversial, and a study has shown that it is ineffective in that role [52].

Coupling ozone with other agents usually increases the PFAS degradation yield. Bubbling ozone in a photoreactor containing a 28 W mercury lamp (254 nm) and the photocatalyst TiO_2, allowed a 4.18 times defluorination increase when compared with the UV/O_3 system [14]. Coupling ozone with H_2O_2 resulted in an enhanced PFAS removing rates [44]. Using ozone/persulfate in pilot-scale experiments, resulted in a overall 77% PFAS removal improvement and a degradation higher than 98% of the long-chain PFAS [46].

2.2.2. UV degradation techniques

UV radiation is sub-divided into four wavelength regions accordingly to its energy: vacuum UV (VUV), 100-200 nm; UVC, 200-280 nm, which includes the standard 254 nm; UVB, 280-315 nm; and, UVC, 315-400 nm. The energy that corresponds to UV ranges that are usually used in water treatment, VUV and UVC, is 646.8 kJ/mol (185 nm) and 471.1 kJ/mol (254 nm), respectively [53]. Also, C-C and C-F bond energies are 347 and 552 kJ/mol, respectively, meaning that PFAS should not be, at least, fully photolyzed by the 254 nm UV radiation, which is the most common used UV source because it is commercially available for water disinfection applications [54].

The direct degradation of PFOA by 254 nm UV lamp is, as expected, limited [52-56]. Relatively high degradation rates (89% degradation and 33% defluorination yields) were only observed with relatively high power xenon-mercury lamp (200 W) and for a relatively high exposition time (72 h) [56]. The degradation under six UVC-254 nm 4 W lamps for 24 hours resulted in 21% degradation and 9% defluorination yields [52].

UV AOP is commonly coupled to hydrogen peroxide to generate the hydroxyl radical (UV/H_2O_2) and the following mechanism is observed [43]:

$$H_2O_2 + h\nu \rightarrow {}^{*}OH \quad (26)$$
$$H_2O_2 + {}^{*}OH \rightarrow HO_2{}^{*} + H_2O \quad (27)$$
$$H_2O_2 + HO_2{}^{*} \rightarrow H_2O + O_2 + {}^{*}OH \quad (28)$$
$${}^{*}OH + {}^{*}OH \rightarrow H_2O_2 \quad (29)$$
$${}^{*}OH + HO_2{}^{*} \rightarrow H_2O + O_2 \quad (30)$$
$$HO_2{}^{*} + HO_2{}^{*} \rightarrow H_2O_2 + O_2 \quad (31)$$

Preprints (www.preprints.org) | NOT PEER-REVIEWED | Posted: 25 April 2023 doi:10.20944/preprints202304.0927.v1

However, as discussed in the previous ozone section, $^{*}OH$ generation methods are generally ineffective in the degradation of PFAS [53]. Consequently useful UV PFAS degradation processes should be based on other reactive radical species besides the hydroxyl radical, like for example in the system UV/persulfate anion ($S_2O_8^{2-}$). Here, the following chain mechanism is obtained upon activation (heat, UV, iron, etc.), that generates the highly reactive sulfate radical (SO_4^{*-}) [13,43]:

$$S_2O_8^{2-} + h\nu \rightarrow 2\ SO_4^{*-} \quad (32)$$

$$H_2O + SO_4^{*-} \rightarrow HSO_4^{-} + {}^{*}OH \quad (33)$$

$$S_2O_8^{2-} + SO_4^{*-} \rightarrow S_2O_8^{*-} + SO_4^{2-} \quad (34)$$

$$^{*}OH + S_2O_8^{2-} \rightarrow S_2O_8^{*-} + OH^{-} \quad (35)$$

$$^{*}OH + {}^{*}OH \rightarrow H_2O_2 \quad (36)$$

$$SO_4^{*-} + {}^{*}OH \rightarrow HSO_5^{-} \quad (37)$$

$$SO_4^{*-} + SO_4^{*-} \rightarrow S_2O_8^{2-} \quad (38)$$

The sulfate radical has a higher oxidation potential (2.5 ~ 3.1 V) and a long lifetime than the hydroxyl radical [13], and demonstrated to be effective in the PFOS and PFOA degradation [57-61]. Indeed, the activation of persulfate by UV-visible light from a xenon-mercury lamp (200 W – 220 to 460 nm) in an acid solution (pH = 3.0 – 3.1) containing PFOA (1.35 mM) resulted in its complete degradation in 4 hours, and its transformation into fluoride, CO_2 and short-chained PFCA [57]. The activation of persulfate using hot water (60 to 80 ºC) successfully degraded hydroperfluorocarboxylic acids (H-PFCAs) (371–392 microM), achieving 96.7 to 98.2% mineralization after 6h [58]. A similar temperature (85 ºC) activated persulfate procedure was used with PFOA (200 nanog/L) and, after 30 hours, a 93.5% degradation with 43.6% of F^{-} yield was observed, together with the detection of shorter chain length compounds ($C_6F_{13}COOH$, $C_5F_{11}COOH$, C_4F_9COOH and C_3F_7COOH) [59] – this study also showed that lowering the pH and the temperature reduces the degradation efficiency. Several activators for persulfate were compared for the degradation of PFOS (0,186 mM) and the following order were observed: hydrothermal (22,52% defluorination efficiency, 12 hours) > UV (254 nm) > Fe^{2+} > ultrasound [60]. Figures 2 and 3 shows a hypothesis for the mineralization mechanism of PFOS [13].

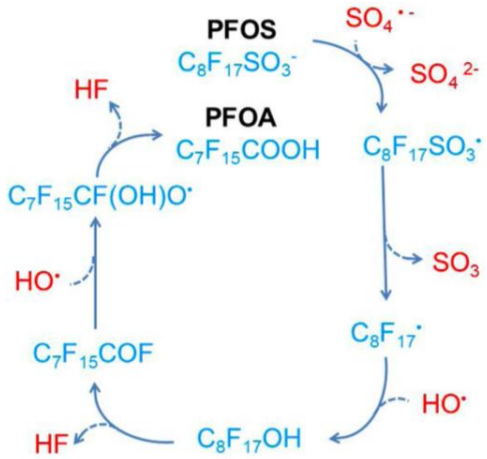

Figure 3 – Proposed mechanisms for the conversion of PFOS to PFOA in the per- sulfate-based system. Adapted with permission from reference [13]. Copyright {2020} Elsevier B.V.

Preprints (www.preprints.org) | NOT PEER-REVIEWED | Posted: 25 April 2023 doi:10.20944/preprints202304.0927.v1

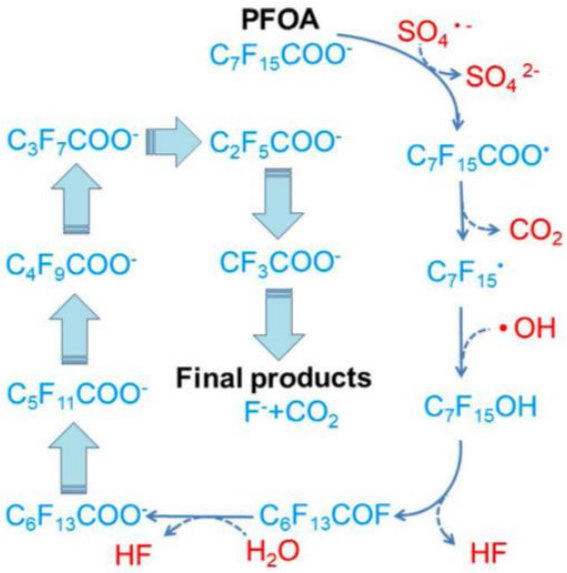

Figure 4 - Proposed pathway for PFOA decomposition in the persulfate-based system. Adapted with permission from reference [13]. Copyright {2020} Elsevier B.V.

2.2.3. Heterogeneous photocatalysis

Using titanium dioxide (TiO_2) as a typical heterogeneous photocatalyst and semiconductor, an AOP based on heterogeneous photocatalysis exposed to ultraviolet and/or visible light has the following mechanism of reactive substances production [43]:

$TiO_2 + h\nu \rightarrow TiO_2 (e_{CB^-} + h_{VB^+})$ (39)
$TiO_2(h_{VB^+}) + H_2O \rightarrow TiO_2 + H^+ + {}^\bullet OH$ (40)
$TiO_2(h_{VB^+}) + OH^- \rightarrow TiO_2 + {}^\bullet OH$ (41)
$TiO_2(e_{CB^-}) + O_2 \rightarrow TiO_2 + O_2^{\bullet-}$ (42)

After TiO_2 absorption, an electron (e_{CB^-}) in the valence band is transferred to the conduction band, leaving a hole in the valence band (h_{VB^+}). A typical example of the application of TiO_2 for PFAS treatment was when an iron halogenide UV lamp (500 W, 95 W/m^2, 315-400 nm) irradiated a suspension of a commercial TiO_2 sample, at a concentration of 0.66 g/L, and it degraded 4 mM PFOA following a pseudo-first order kinetics in the first 4 hours, with an apparent rate constant of 0.1296 h^{-1} [62]. This study also detected shorter perfluorinated carboxylic acids, $C_nF_{2n+1}COOH$ (n=1–6) as intermediates and fluoride anion, which reacted with the surface of the photocatalyst and affected its efficiency.

Doping TiO_2 with metal ions improve the photocatalytic efficiency of the semiconductor by producing traps in the molecular orbitals that capture the electrons and holes, reducing the electron-hole recombination, making them more available to react with organic molecules leading to their degradation [63]. Copper-doped TiO_2 upon exposition to UV light (245 nm, 200 W) catalyzed the decomposition of PFOA after 12 hours with an apparent rate constant of 0.186 h^{-1} and a defluorination rate constant of 0.462 mg/L h^{-1} [63]. The decomposition of the PFOA into fluoride ions and shorter PFCA, such as $C_6F_{13}COOH$, $C_5F_{11}COOH$, C_4F_9COOH, C_3F_7COOH, C_2F_5COOH and CF_3COOH, was observed.

A material produced from low cost commercial activated carbon and TiO_2 was prepared, named Fe/TNTs@AC, having both synergistic adsorption and photocatalytic capabilities [64]. This material (in a concentration of 4 g/L), upon exposition for 4 h under UV irradiation (254 nm, 21 mW cm^{-2}), was able to degrade more than 90% of PFOA with

Preprints (www.preprints.org) | NOT PEER-REVIEWED | Posted: 25 April 2023 doi:10.20944/preprints202304.0927.v1

a 62% mineralization to fluoride ions in the pH range between 4 and 8. Using selective scavengers it was concluded that the hole h_{VB}+ is the important player in the PFOA degradation - $^{*}OH$ and O_2^{*-} did not have a particularly active role [64].

New material semiconductors, with improved photocatalytic efficiencies, particularly in the visible wavelength range, have been prepared based on bismuth [17,65,66]. Based on the so called "concentrate and destroy" strategy, a bismuth phosphate was coupled to carbon spheres (CS) resulting in the composite BiOHP/CS [17]. This composite (1 g/L) was able to quantitatively adsorb PFOA (initial concentration of 200 microg/L at pH=7) in 2 hours, and achieve its almost complete decomposition in 4 hours when irradiated by a UV light (18 W low-pressure Hg lamp, 254 nm, 21 mW/cm^2).

Bismuth oxohalides (BiOX, X – F, Cl, Br and I) are typical photocatalysts, and the BiOI has a narrow bandgap (e.g. 1.7–1.9 eV) which allows its used in the visible wavelength range, and several composites with it have been proposed for the treatment of PFAS in water [65,66]. The photocatalyst BiOI@Bi_5O_7I (0.5 g/L) degrades PFOA (15 mg/L) under simulated solar light with a rate constant of 0.247 h^{-1} (removes about 60% of the organic carbon on 6 hours of irradiation) [65]. The role in the PFOA decomposition of the reactive species $^{*}OH$, O_2^{*-} and h_{VB}+ were assessed using selective scavengers, and all the species were active in that mechanism. This study also showed that PFOA was decomposed by stepwise losing CF_2 units (Figure 5). Bi_5O_7I/ZnO microspheres were used in PFOA degradation analysis when irradiated with simulated visible light (400 W Xe lamp with a 420 nm cutoff filter), and a degradation rate constant of 0.013 h^{-1} was obtained [66]. This work demonstrated that the degradation of the PFOA begun by the most reactive carboxylic acid group of PFOA, which was vulnerable to attack by the h_{VB}+, followed by the successive elimination of CF_2 units.

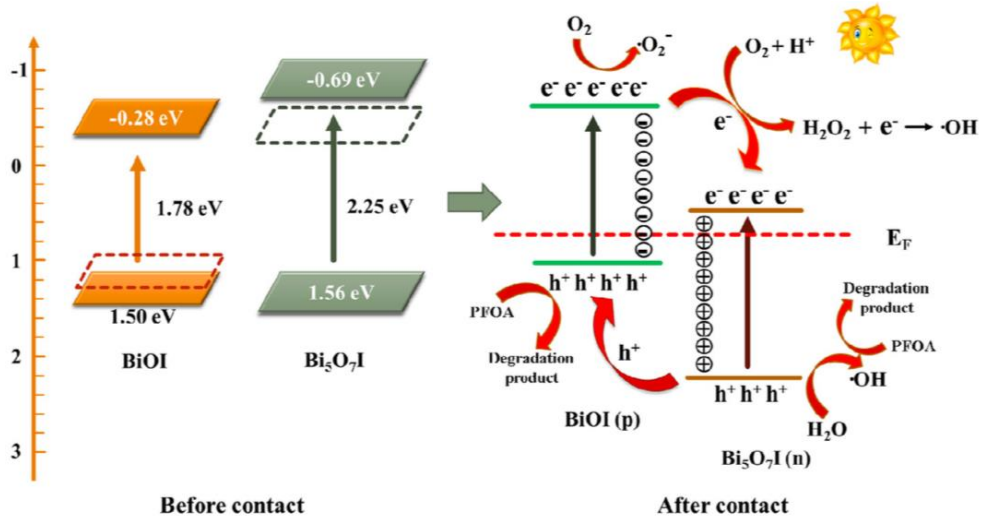

Figure 5 - Proposed photocatalytic mechanism of PFOA in BiOI@Bi_5O_7I *p-n* heterojunction photocatalytic system. Adapted with permission from reference [65]. Copyright {2019} Elsevier B.V.

Taking into consideration that the potential quantity of water to be treated for PFAS is enormous, photocatalyst design must take into consideration environmental and social/economical sustainability issues. A low cost and sustainable zero-valence iron (PVP/Fe^0) was used as photocatalyst for the degradation under UV radiation (14 UVC light bulbs, 8 W each, centered at 254 nm, 4.24 mW/cm^2) of a mixture of PFOA, PFOS and perfluorononanoic acid (PFNA) in real wastewater from WWTP [18]. The degradation percentages were (0.5 microg/L of each PFAS at pH=3) 90, 88 and 43% for PFAN, PFOS and PFOA, respectively.

Preprints (www.preprints.org) | NOT PEER-REVIEWED | Posted: 25 April 2023 doi:10.20944/preprints202304.0927.v1

3. Nanomaterials based AOP and ARP

The incorporation of nanomaterials in nearly all the AOP has already been done with promising results [67]. Due to its high SSA and specific designed surface, nanomaterials act as AOP catalysts, resulting in an increased production of reactive species under mild experimental conditions, improving degradation yields for lower contact times. Typical examples of these catalysts are those used in heterogeneous Fenton-like processes for the production of hydroxyl radical from hydrogen peroxide (Figure 6) using, mainly, iron-based nanomaterials [67].

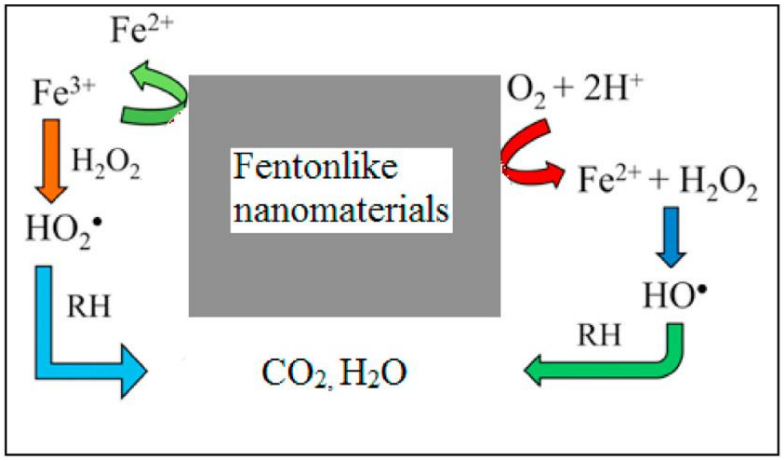

Figure 6 - Schematic representation of the action of Fenton-like nanomaterials in the degradation of organics. Fe^{2+}/Fe^{3+} redox couple generates the reactive free radicals involved in the degradation of toxic pollutants. Adapted with permission from reference [67]. Copyright {2021} Elsevier B.V.

Although with some identified limitations as previously discussed, ARP and AOP show great potential for the treatment of water, either for human consumption and wastewater, contaminated with PFAS . However, the performance and the sustainability of those processes must be improved, because fast and high degradation yields processes must be developed, taking into consideration sustainability issues like raw materials extraction and environmental impacts. Taking into consideration the increased reactivity, markedly lower mass content and large SSA, nanomaterials can definitely contribute to this optimization evolution of the PFAS treatment classical technologies.

3.1. Previous reviews

Three previous reviews have been published about the use of nanomaterials in PFAS treatment technologies, and have discussed publications until the year 2021 [19,21,22]. The general analysis of these reviews shows that nanomaterials have been proposed with two main functions in the treatment technologies, general adsorption (removal of PFAS from the water and its concentration in the nanomaterial) and heterogeneous photocatalysis degradation of PFAS AOP.

The majority of the proposed nanomaterials used for adsorption water treatment technologies use carbon nanotubes (CNT) [68]. The use of carbon-based nanomaterials results from good performance of the well known granular activated charcoal (GAC), which implementation is widespread for the adsorption of micropollutants, including PFAS, in classical water treatment technologies [69]. Also, CNT are being proposed as highly promising materials for water treatment technologies [68], but its toxicity and potential heath risks may compromise that application [70], and it is mandatory the re-

 doi:10.20944/preprints202304.0927.v1

search on alternatives. A carbon-based nanomaterial, with much better sustainability characteristics than CNT, are carbon dots [71,72].

Metal oxides nanoparticles are also used as nanoadsorbent platforms for PFAS because they have high SSA and many surface functional groups [22]. Because PFAS soluble in water have a negative charge, the adsorption is maximized when the pH is lower than the point of zero-charge (PZC) of the oxide, namely: Al_2O_3, 7.3; Fe_2O_3, 7.6; and TiO_2, 5.4 [73]. Besides the pH, the SSA and the surface hydroxyl density (SHD) are critical factors in the PFAS adsorption efficiency of the metal oxides, and the SSA (m^2/g) and SHD (micromol/m^2) are, respectively: Al_2O_3, 198 and 31.2; Fe_2O_3, 41.7 and 21.0; TiO_2, 64.1 and 35.5; and, SiO_2, 278 and 18.3 [73]. Also, the formation of inner-sphere complexes at the surface of the metal ions by of metal cations increases the adsorption capacity [22,73]. Other experimental factors contribute to the adsorption inhibition, namely the presence of negatively charged polymers, like dissolved organic matter, that will compete with PFAS for the adsorption sites, and the agglomeration of the adsorbent nanoparticles. Nano alumina, hematite and goethite showed better adsorption characteristics.

Semiconductor nanometal oxides, like TiO_2 (band gap - 3.0–3.2 eV, ~400 nm), In_2O_3 (band gap - ~2.9 eV, ~428 nm) and Ga_2O_3 (band gap – 4.8 eV, 258 nm) have being proposed as photocatalysts in UV AOP [19,21]. Indeed, some of these nanomaterials correspond to the size reduction towards the nanometer dimensions of some of the bulk photocatalysts that have been used in classical UV AOP, and previous discussed in section 2.2.3. Among the semiconductor nanometal oxides, In_2O_3 photocatalysts were shown to have the highest potential for PFAS degradation due to its SSA and the type and amounts of reactive species that are generated upon UV irradiation [19]. Photocatalytic degradation efficiencies can be improved by doping metal oxides with CeO_2 and noble metals (Ag, Pt, Pd) [22].

However, due to the costs and limited environmental resources, the use in large scale plants of the metals described in the previous paragraph, raises severe sustainability concerns. As an alternative, cheaper and more abundant metals are being used for PFAS degradation, like for example Zn (mainly as ZnO), Fe (mainly as Fe^0) and Mn (mainly as Mn_2O_3) [22]. Significant PFAS degradation is observed when these nanometals/nanometal oxides are coupled with UV/ozone or hydrogen peroxide, either under UV or visible radiation [22].

The most important characteristic of nanomaterials that makes them suitable to be coupled to ARP/AOP is their versatility. They can be designed to have a particular functionality, or several functionalities, with residual mass of resources, when compared with bulk materials. Moreover, taking into consideration their extraordinary high SSA, it results into higher reactivity.

Although the research in nanomaterials applications in the treatment of PFAS in water was oriented independently into two main lines, adsorption and degradation, the next step is the combination of these two functionalities in only one nanoparticle. Indeed, the strategy of "concentrate and destroy", discussed above in section 2.2.3, is the next step behind nanomaterials design for ARP/AOP for PFAS treatment.

3.2. Advances in concentration strategies of PFAS

Environmental sustainability concerns were translated into the proposal of technologies based on biological systems and nanomaterials [73-75]. A Renewable Artificial Plant for in-situ Microbial Environmental Remediation (RAPIMER) was developed from chemical modified lignocellulosic biomass (Figure 7) [73]. RAPIMER is a nanomaterial, based on cellulose and lignin, that enables an efficient PFAS adsorption, provides a

Preprints (www.preprints.org) | NOT PEER-REVIEWED | Posted: 25 April 2023 doi:10.20944/preprints202304.0927.v1

support for fungus and bacteria that will decompose PFAS, and support the expression of redox enzymes to degrade PFAS. RAPIMER has finer nanometric (2.35 nm) fiber structure, which results in a high SSA, and the negatively charged cellulose nanofibrils (hydrophilic) and the positively charged lignin (hydrophobic) generated a 3D amphiphilic environment, allowing PFAS strong adsorption due to charge attraction and hydrophobic interaction. RAPIMER has a PZC of 8.22 and adsorption decreases for pH below than 8. Low concentrations of PFOA and PFOS (1 microg/L) in complex solutions were removed by RAPIMER at efficiencies of 99% or higher. The adsorbed PFAS inside RAPIMER were subjected to bioremediation.

PFAS suffer bioremediation in anaerobic reactor where carbon materials, including CNT, were supplemented as electron drivers [74]. Biological methods for PFAS environmental removal are being investigated [75], and are characterized for being cost-effective, eco-friendly and with simple operation. Nanomaterials (nanobiochar, CNT, nanometal oxides) are being included in biological technologies as adsorbent nanoplatforms.

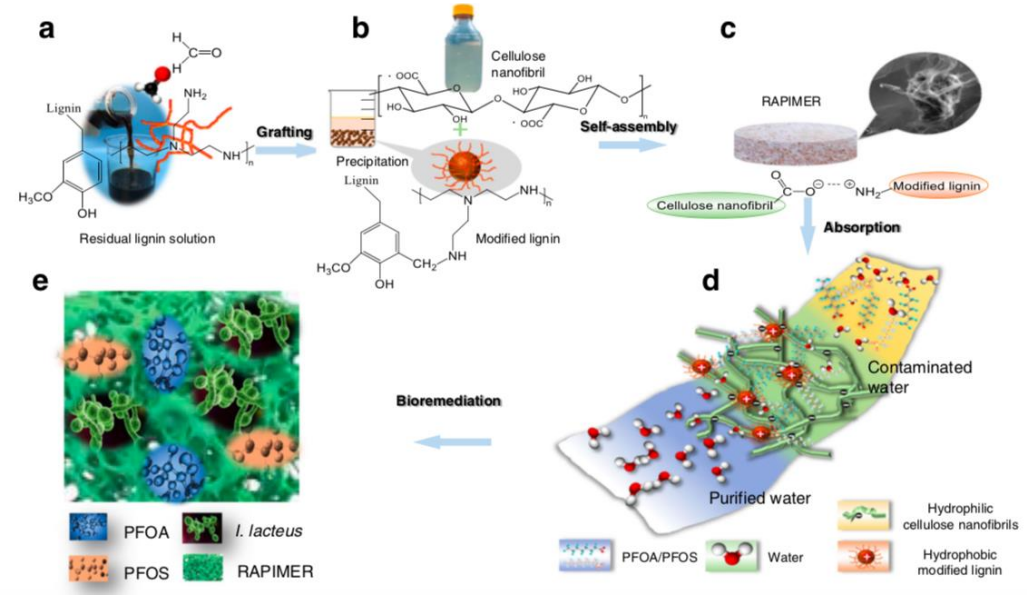

Figure 7 - The design strategy, fabrication process, chemical adsorption, and fungus degradation scheme of the RAPIMER system. a) Corn stover residual lignin solution and selective graft reaction using formaldehyde and polyethylenimine to produce positively charged modified lignin particles. b) Corn stover derived cellulose nanofibrils prepared by TEMPO-oxidation method and modified lignin chemical structure. c) The modified lignin and nanocellulose nanofibrils formed RAPIMER composite through self-assembly by the formation of carboxylic acid/amine interaction. d) PFAS adsorption by the RAPIMER composite. e Fungal bioremediation through co-metabolism and biodegradation of PFAS and RAPIMER system. Adapted from reference [73].

Foam fractionation technologies (FFT) are being proposed as pre-treatment of water to remove soluble PFAS, and for producing low-volume high concentrated solutions for subsequent destruction [76-78]. Long-chain PFAS are usually removed with high efficiencies (>90%), while short-chain PFAS are removed with low efficiencies (<30%) [76]. Although nanomaterials have not been included in the FFM formulations for PFAS concentration, these technologies are also used for nanomaterials (silica nanoparticles and CNT) removal from wastewater [79]. Taking into consideration the active role of nanomaterial in the adsorption/degradation of PFAS based in several AOP, the coupling of FFT for PFAS treatment with designed nanomaterials is an open window of research.

Preprints (www.preprints.org) | NOT PEER-REVIEWED | Posted: 25 April 2023 doi:10.20944/preprints202304.0927.v1

CNT, both single-walled (SWCNT) and multi-walled (MWCNT), continue to be proposed as adsorbent platforms for PFAS, but SWCNT show better adsorption performances due to the lower SSA of MWCNT [80]. Also, the modification of CNT with nano-$MgAl_2O_4$ has been proposed as an improved adsorbent for PFAS (100 ppb) allowing 99% removal after 3 hours and 100% in 3.5 hours [81]. The size of the nanocomposite $MgAl_2O_4$@CNT was 80 to 120 nm, with a SSA of 149.41 m^3/g, a pore volume of 0.27 cm^3/g and a pore size of 9.69 nm. The nanocomposite adsorbs PFAS by hydrophobic and electrostatic interactions and can be used at mild alkaline solutions.

Metal-organic frameworks (MOF), which are innovative nanopores ordered materials with high SSA and pore volumes, have shown an increased application for PFAS adsorption in the last years [80,82,83].

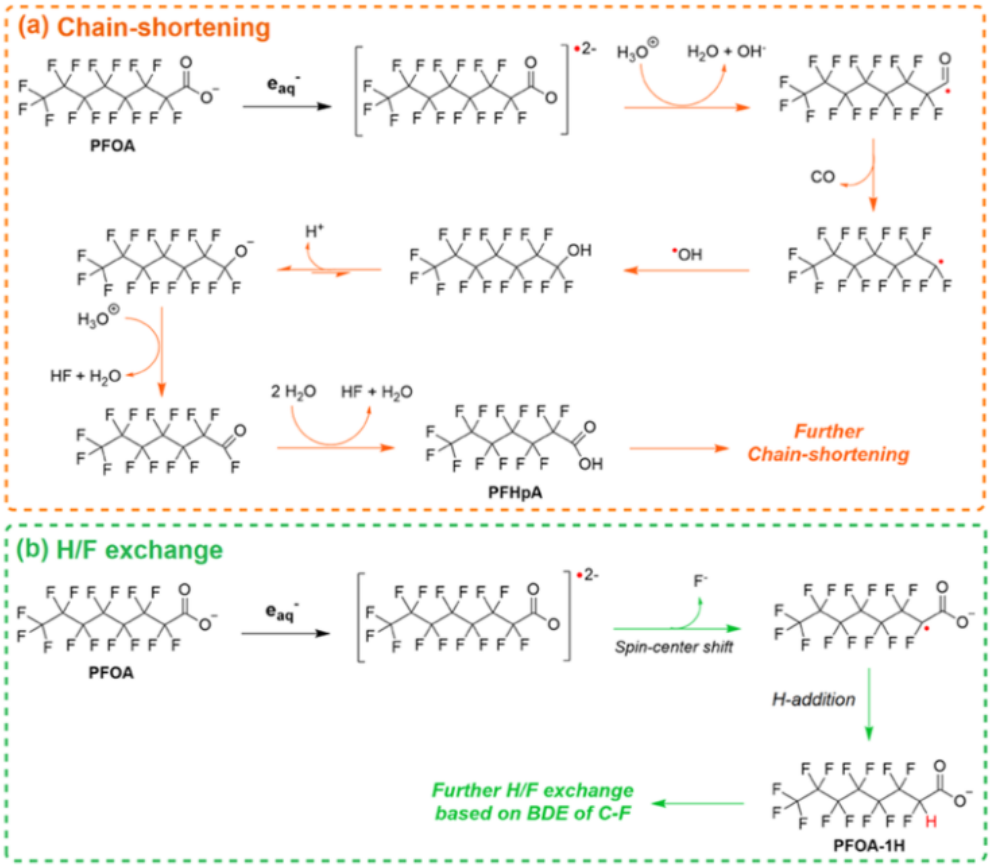

Figure 8. Plausible reaction mechanisms of (a) Chain-Shortening and (b) H/F Exchange in the degradation of PFOA in the MIL-125-NH_2 MOF system. Adapted with permission from reference [83]. Copyright {2022} American Chemical Society.

3.3. Advances in PFAS treatment technologies

Besides the potential as adsorptive material for PFAS, MOF, and particularly the titanium based MIL-125-NH_2, was used as a photocatalyst for degradation of PFOA under a 450 W mercury lamp [83]. After 24 hours irradiation, 98.9% degradation and 66.7% defluorination rate of PFOA were obtained. Glucose, that is a critical factor for the degradation, was used as non-hazardous sacrificial reductant, where it acts as a h_{VB}^+ scavenger. The degradation mechanism involves e_{aq}^- and oxidizing reactive species (Figure 8).

Preprints (www.preprints.org) | NOT PEER-REVIEWED | Posted: 25 April 2023 doi:10.20944/preprints202304.0927.v1

2D nanomaterials, Pt/$La_2Ti_2O_7$ nanoplates and BiOF nanosheets, were prepared to be used as photocatalyst of PFOA degradation [84,85]. $La_2Ti_2O_7$ has a layered perovskite structure and is known to decompose water into hydrogen and oxygen by photocatalytic reduction under UV irradiation [84]. Pt was dispersed on the photocatalyst to improve catalytic activity. Irradiating a PFOA water solution without oxygen (bubbling nitrogen) using an UV light (254 nm, 1 mW cm^{-2}), in the presence of Pt/$La_2Ti_2O_7$ and methanol, as an electron donor, it was observed a 40% degradation after 180 minutes and 50% degradation after 12 hours. BiOF nanosheets photocatalyst were prepared with different amounts of ethylene glycol taking into consideration that surface defects and/or exposed reactive facets should improve the photocatalytic performance [85]. The sample 50%-EG BiOF, under UV light, catalyzes the almost complete removal of PFOA and 56.8% removal of TOC.

One dimensional titanate nanotubes (TNT) are TiO_2 derivatives that have an uniform crystalline and scrolled tubular structure [TiO_6], large SSA and high pore volume, good ion-exchange ability, high photoelectric conversion properties and, some derivatives, have high visible light response [86]. Figure 9 shows a scheme of the formation of TNT. Upon solar irradiation of TNT, a similar mechanism of reactive substances production to TiO_2 irradiated with UV, eq. (39) to (42), is observed. However, raw TNT, cannot be used for PFAS adsorption (and eventually destruction) because the negative and hydrophilic surface of TNT repel the negative water soluble PFAS. This limitation was overcome by doping TNT with photoactive metal oxides and by using activated charcoal (AC) as supports (Metal/TNT@AC) [64,87-89]. These modifications allowed the development of PFAS "concentrate and destroy" technologies [64,87-89].

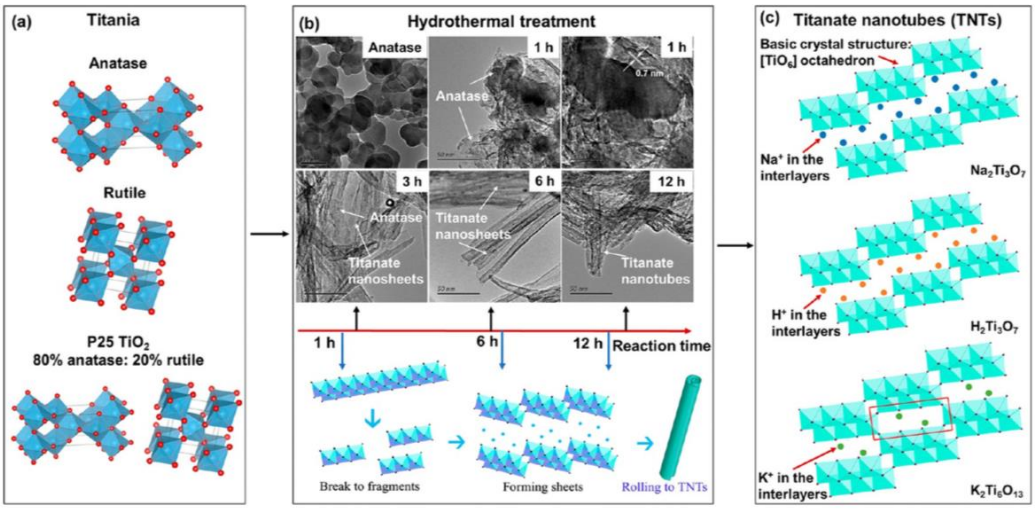

Figure 9. (a) Crystalline structures of TiO_2 (red balls: O, dusty blue balls: Ti); (b) TEM morphologies of the original anatase and intermediate materials with different hydrothermal reaction times of 1–12 h, and schematic diagram of TNTs formation; (c) crystalline structures of typical TNTs (purple balls: O; blue balls: Na; orange balls: H; green balls: K). Adapted with permission from reference [86]. Copyright {2022} American Chemical Society.

Ga/TNT@AC [87,88] and Bi/TNT@AC [89] were prepared and used for adsorption and destruction of PFAS. The UV irradiation (210 W/m^2) of Ga/TNT@AC (0,12 g) allowed 75% degradation and 66.2% mineralization of PFOS (100 microg/L, pH=7) within 4 hours [87,88]. The photoactivity of Ga/TNT@AC was attributed to oxygen vacancies which suppresses recombination and facilitates superoxide radical. Both, the hole h_{VB}+ and $O_2^{\bullet-}$, played an important role in the PFOS degradation. The UV irradiation (210 W/m^2) of Bi/TNT@AC (1 g/L) allowed 70% degradation and 42.7% mineralization of GenX (100 microg/L, pH=7) within 4 hours [89] – GenX is the ammonium salt of hexafluoropropylene oxide dimer acid, and has been used as a PFOA replacement. The photoactivity of Bi/TNT@AC was attributed to hydroxyl radical and the hole h_{VB}+.

Preprints (www.preprints.org) | NOT PEER-REVIEWED | Posted: 25 April 2023 doi:10.20944/preprints202304.0927.v1

Iron-based nanocomposites were proposed as adsorbents/catalysts for PFAS removal and degradation [18,20,90]. The removal of PFAS in wastewater effluents was successful using zero valence iron nanoparticles coupled to UV light [18]. The degradation of PFAS in wastewater effluents were lower than in deionized water and the degradation was higher at acid pH values (pH=3) – after 2 hours, degradation rates of 90%, 88% and 46% were obtained for PFNA, PFOS and PFOA. Ferric hydroxide nanoparticles were synthesized *in situ* using ozone and the nanoparticles used for PFAS removal [20]. Although no PFAS destruction analysis was done, the adsorbent capacity of these nanoparticles was higher than conventional adsorbents which, taking into consideration iron reactivity, have potential for the development of a "concentrate and destroy" process. An iron-clay(montmorillonite)-cyclodextrin(β–CD)-DFB (decafluorobiphenyl) was synthesized, and the iron-clay segment has a heterogeneous Fenton catalyst function, while the CD-DFB was used as a surface-confinement for PFAS molecules [90]. This composite adsorb >90% and oxidize >70% long-chain PFAS and showed worse performance for short-chain PFAS. In the case of PFOA and PFOS, a 65% degradation was observed within 10 minutes.

New applications of TiO_2 in novel photocatalysts are being investigated, like the composite resulting from the calcination of boron nitrite (BN) with TiO_2, BN/TiO_2 [91]. The BN/TiO_2 composite is more photoactive than the two precursors under UV light for PFOA, degrading 15 times faster than TiO_2, with the active reactive species being photogenerated holes. Also, the lifetime of PFOA in outdoor experiments under natural sunlight, and in deionized water, was of 1.7 hours.

An UV-Fenton reaction catalyzed by Fe_3O_4 nanoparticles was proposed for PFAS destruction [92]. Fenton AOP involves the oxidation of a ferrous ion (Fe^{2+}) by hydrogen peroxide in the presence of UV radiation to promote the formation of reactive oxygen species, $^{*}OH$ and HO_2^{*} radicals [91]:

$$Fe^{2+} + H_2O_2 \rightarrow Fe^{3+} + {}^{*}OH + OH^{-} \quad (43)$$

$$Fe^{3+} + H_2O_2 \rightarrow Fe^{2+} + HO_2^{*} + H^{+} \quad (44)$$

$$2H_2O_2 \rightarrow {}^{*}OH + HO_2^{*} + H_2O \quad (45)$$

The UV Fenton system used six 15 W UV-C bulbs (wavelength 254 nm, 120 μJ cm^{-2}), nano-magnetite (20–30 nm) and different pH values and hydrogen peroxide concentrations [92]. The samples were irradiated from 5 minutes to one-hour periods and left reacting for 24 hours before analysis - Figure 9 resumes the observed degradation efficiencies of the tested PFAS under this system. About 90% degradation rates were observed, with the exception for the short-chain PFAS where much lower degradation percentages occur. Both, nano-magnetite and H_2O_2, contribute to the PFAS destruction, suggesting that ROS and the adsorption of PFAS in the surface of magnetite contribute to their destruction mechanism.

Preprints (www.preprints.org) | NOT PEER-REVIEWED | Posted: 25 April 2023 doi:10.20944/preprints202304.0927.v1

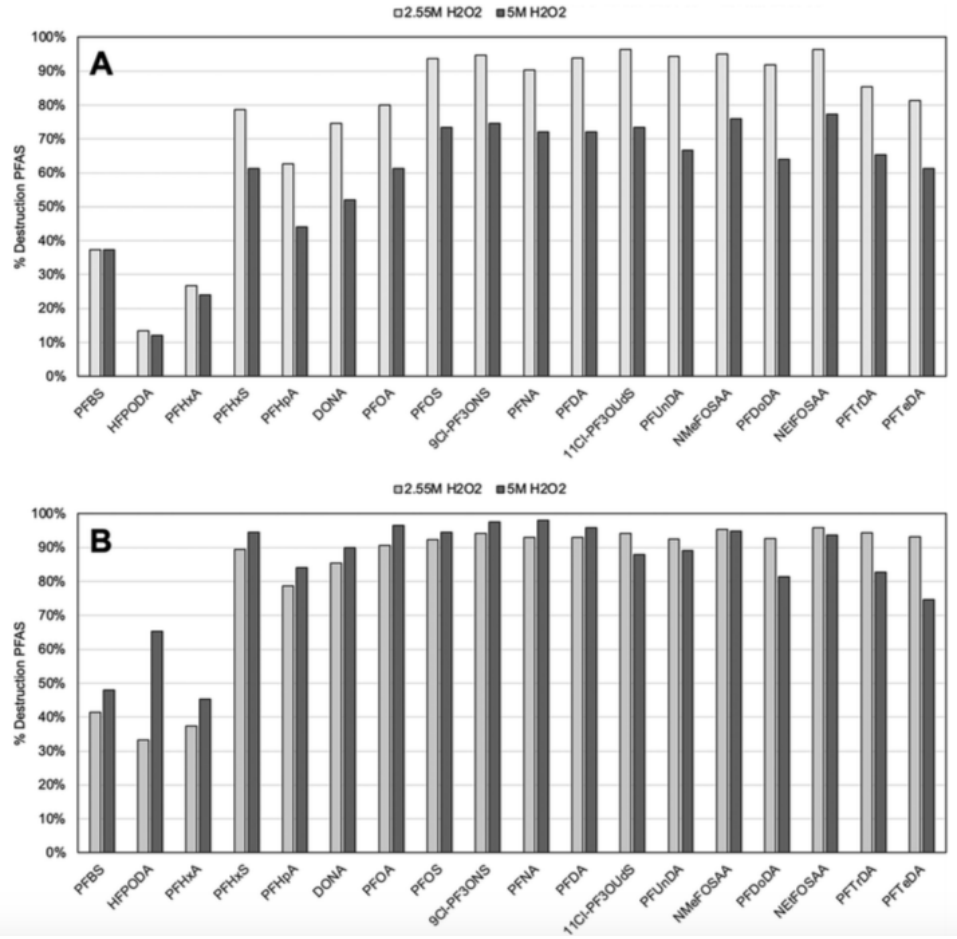

Figure 10. Percent destruction of 18 PFAS species at (A) pH 7 and (B) pH 9 and two concentrations of H_2O_2. All samples were prepared with 1000 ppm Fe_3O_4 and underwent 30 minutes of UV-C exposure. Instrumental analysis measurement uncertainty for detected concentration (in units of ppt) are as follows: PFBS – 23.2%; HFPODA* – 28.3%; PFHxA – 21.8%; PFHxS – 21.6%; PFHpA – 23.2%; DONA* – 22.9%; PFOA – 22.5%; PFFOS – 25.2%; 9Cl-PF3ONS – 22.3%; PFNA – 21.5%; PFDA – 23.2%; 11Cl-PF3OUdS* – 25.9%; PFUnDA – 22.8%; NMeFOSAA – 27.1%; PFDoDA – 24.4%; NEt-FOSAA* – 25.8%; PFTrDA – 26.5%; PFTeDA – 21.6%. *These PFAS species are branched, which may impact their reactivity when compared with the linear compounds. Adapted with permission from reference [91]. Copyright {2022} The Royal Society of Chemistry.

4. Perspectives

This review showed that classical advanced oxidation and/or reduction processes for water treatment can be used for the degradation of PFAS. Moreover, it was discussed the advantages of coupling those processes with specific designed nanomaterials following the "concentrate and destroy" strategy. However, research on the coupling of nanomaterials and AOP/ARP is still highly insufficient, because results are only available for heterogeneous catalysts AOP.

Indeed, the next designed strategy for the PFAS nanomaterials/AOP for water treatment must be a "super-concentration/high-yield-destruction/sustainable" approach. This can be achieved using porous carbon based nanomaterials, synthesized from biogenic waste, as the basis for a nanocomposite containing active dopants that will catalyze reactive molecular species overproduction in an ARP/AOP.

The research on new advanced processes technologies will open new treatment windows for PFAS in water and for the development of new nanomaterials. For example, recently [93], it was observed that the chlorine radicals (Cl^* and Cl_2^{*-}) play an important role in the degradation of PFOA. Chlorine radicals are generated by UV/Chlorine tech-

nologies. Also, it was discovered that PFCA can be mineralized under low temperature conditions in the presence of hydroxide anion [94]. Indeed, the decarboxylation of PFCA occur in polar non-protic solvent, when the hydroxide anion is present, resulting in the production of a carbanion that undergoes decomposition. Nanoparticle design for non-aqueous solvents is still a challenge, but encouraging perspectives are open with this last discover.

Author Contributions: Conceptualization, I.M.S.C., L.P.d.S. and J.E.S.; writing—original draft preparation, I.M.S.C. and J.E.S.; writing—review and editing, L.P.d.S. and J.E.S.; supervision, L.P.d.S. and J.E.S.; funding acquisition, L.P.d.S. and J.E.S. All authors have read and agreed to the published version of the manuscript.

Funding: The Portuguese "Fundação para a Ciência e Tecnologia" (FCT, Lisbon) is acknowledged for funding of project PTDC/QUI-QFI/2870/2020, R&D Units CIQUP (UIDB/000081/2020 and UIDP/00081/2020) and the Associated Laboratory IMS (LA/P/0056/2020). L.P.d.S. also acknowledges FCT for funding under the Scientific Employment Stimulus (CEECINST/00069/2021).

Conflicts of Interest: The authors declare no conflict of interest. The funders had no role in the design of the study; in the collection, analyses, or interpretation of data; in the writing of the manuscript; or in the decision to publish the results.

References

1. Vo, H.N.P.; Ngo, H.H.; Guo, W.; Nguyen, T.M.H.; Li, J.; Liang, H.; Deng, L.; Chen, Z.; Nguy, T.A.H. Poly- and perfluoroalkyl substances in water and wastewater: A comprehensive review from sources to remediation. Journal of Water Process Engineering 2020, 36, 101393.
2. Domingo, J.L.; Nadal. M. Human exposure to per- and polyfluoroalkyl substances (PFAS) through drinking water: A review of the recent scientific literature. Environmental Research 2019, 177, 108648.
3. http://www.pops.int/TheConvention/ThePOPs/tabid/673/Default.aspx (19/march/2023)
4. Teymoorian, T.; Munoz, G.; Vo Duy, S.; Liu, J.; Sauvé. S. Tracking PFAS in Drinking Water: A Review of Analytical Methods and Worldwide Occurrence Trends in Tap Water and Bottled Water. ACS Environmental Science and Technology Water 2023, 3, 246−261.
5. Wanninayake. D.M. Comparison of currently available PFAS remediation technologies in water: A review. Journal of Environmental Management 2021, 283, 111977.
6. Leung, S.C.; Shukla, P.; Chen, D.; Eftekhari, E.; An, H.; Zare, F.; Ghasemi, N.; Zhang, D.; Nguyen, N.T.; Li, Q. Emerging technologies for PFOS/PFOA degradation and removal: A review. Science of the Total Environment 2022, 827, 153669.
7. Araújo, R.J.; Rodríguez-Hernandéz, J.A.; González-González, R.B.; Macias-Garbett, R.; Martínez-Ruiz, M.; Reyes-Pardo, H.; Martínez, S.A.; Parra-Arroyo, L.; Melchor-Martínez, E.M.; Sosa-Hernández, J.E.; Coronado-Apodaca, K.G.; Varjani, S.; Barceló, D.; Iqbal, H.M.N.; Parra-Saldívar, R. Detection and Tertiary Treatment Technologies of Poly-and Perfluoroalkyl Substances in Wastewater Treatment Plants. Frontiers in Environmental Science 2022, 10, 864894.
8. Ateia, M.; Alsbaiee, A.; Karanfil, T.; Dichtel. W. Efficient PFAS Removal by Amine-Functionalized Sorbents: Critical Review of the Current Literature. Environmental Science and Technology Letter 2019, 6, 688−695.
9. Park, M.; Wu, S.; Lopez, I.J.; Chang, J.Y.; Karanfil, T.; Snyder. S.A. Adsorption of perfluoroalkyl substances (PFAS) in groundwater by granular activated carbons: Roles of hydrophobicity of PFAS and carbon characteristics. Water Research 2020, 170, 115364.
10. Militao, I.M.; Roddick, F.A.; Bergamasco, R.; Fan. L. Removing PFAS from aquatic systems using natural and renewable material-based adsorbents: A review. Journal of Environmental Chemical Engineering 2021, 9, 105271.
11. Yadav, S.; Ibrar, I.; Al-Juboori, R.A.; Singh, L.; Ganbat, N.; Kazwini, T.; Karbassiyazdi, E.; Samal, A.K.; Subbiah, S.; Altaee. A. Updated review on emerging technologies for PFAS contaminated water treatment. Chemical Engineering Research and Design 2022, 182, 667–700.
12. Dixit, F.; Dutta, R.; Barbeau, B.; Berube, P.; Mohseni. M. PFAS removal by ion exchange resins: A review. Chemosphere 2021, 272, 129777.
13. Yang, L.; He, L.; Xueb, J.; Ma, Y.; Xie, Z.; Wu, L.; Huang, M.; Zhang. Z.; Persulfate-based degradation of perfluorooctanoic acid (PFOA) and perfluorooctane sulfonate (PFOS) in aqueous solution: Review on influences, mechanisms and prospective. Journal of Hazardous Materials 2020, 393,122405.
14. Huang, J.; Wang, X.; Pan, Z.; Li, X.; Ling, Y.; Li. L. Efficient degradation of perfluorooctanoic acid (PFOA) by photocatalytic ozonation. Chemical Engineering Journal 2016, 296, 329–334.
15. Kim, J.;Xin, X.; Mamo, B.T.; Hawkins, G.L.; Li, K.; Chen, Y.; Huang, Q.; Huang. C. Occurrence and Fate of Ultrashort-Chain and Other Per- and Polyfluoroalkyl Substances (PFAS) in Wastewater Treatment Plants. ACS EST Water 2022, 2, 1380−1390.
16. Manz, K.E.; Kulaots, I.; Greenley, C.A.; Landry, P.J.; Lakshmi, K.V.; Woodcock, M.J.; Hellerich, L.; Bryant, J.D.; Apfelbaum, M.; Pennell. K.D. Low-temperature persulfate activation by powdered activated carbon for simultaneous destruction of perfluorinated carboxylic acids and 1,4-dioxane. Journal of Hazardous Materials 2023, 442,129966.

17. Xu, T.; Zhu, Y.; Duan, J.; Xi, Y.; Tong, T.; Zhang, L.; Zhao. D. Enhanced photocatalytic degradation of perfluorooctanoic acid using carbon-modified bismuth phosphate composite: Effectiveness, material synergy and roles of carbon. Chemical Engineering Journal 2020, 395, 124991.
18. Xia, C.; Lim, X.; Yang, H.; Goodson, B.M.; Liu. J. Degradation of per- and polyfluoroalkyl substances (PFAS) in wastewater effluents by photocatalysis for water reuse. Journal of Water Process Engineering 2022, 46, 102556.
19. Zhang, W.; Zhang, D.; Liang. Y. Nanotechnology in remediation of water contaminated by poly- and perfluoroalkyl substances: A review. Environmental Pollution 2019, 247, 266-276.
20. Zhang, J.; Pang, H.; Gray, S.; Ma, S.; Xie, Z.; Gao. L. PFAS removal from wastewater by in-situ formed ferric nanoparticles: Solid phase loading and removal efficiency. Journal of Environmental Chemical Engineering 2021, 9, 105452.
21. Birch, Q.T.; Birch, M.E.; Nadagouda, M.N.; Dionysiou. D.D. Nano-enhanced treatment of per-fluorinated and poly- fluorinated alkyl substances (PFAS). Current Opinion in Chemical Engineering 2022, 35, 100779.
22. Yin, S.; Villagrán. D. Design of nanomaterials for the removal of per- and poly-fluoroalkyl substances (PFAS) in water: Strategies, mechanisms, challenges, and opportunities. Science of the Total Environment 2022, 831, 154939.
23. Duinslaeger, N.; Radjenovic. J. Electrochemical degradation of per- and polyfluoroalkyl substances (PFAS) using low-cost graphene sponge electrodes. Water Research 2022, 213, 118148.
24. C Fang, C.; Megharaj, M.; Naidu, R. Electrochemical Advanced Oxidation Processes (EAOP) to degrade per- and polyflluoroalkyl substances (PFASs). Journal of Advanced Oxidation Technologies. 2017, 20170014.
25. Trojanowicza, M.; Bojanowska-Czajkaa, A.; Bartosiewicza, I.; Kulisa, K. Advanced Oxidation/Reduction Processes treatment for aqueous perfluorooctanoate (PFOA) and perfluorooctanesulfonate (PFOS) – A review of recent advances. Chemical Engineering Journal 2018, 336, 170–199.
26. Saleh, N.B.; Khalid, A.; Tian, Y.; Ayres, C.; Sabaraya, I.V.; Pietari, J.; Hanigan, D.; Chowdhury, I.; Apul, O.G. Removal of poly- and per-fluoroalkyl substances from aqueous systems by nano-enabled water treatment strategies. Environ. Sci.: Water Res. Technol., 2019,5, 198-208.
27. Cui, J.; Gao, P.; Deng, Y. Destruction of Per- and Polyfluoroalkyl Substances (PFAS) with Advanced Reduction Processes (ARPs): A Critical Review. Environ. Sci. Technol. 2020, 54, 3752−3766.
28. Leonello D.; Fendrich, M.A.; , Parrino, F.; Patel, N.; Orlandi, M.; Miotello, A. Light-Induced Advanced Oxidation Processes as PFAS Remediation Methods: A Review. Appl. Sci. 2021, 11, 8458.
29. Barisci, S.; Suri, R. Occurrence and removal of poly/perfluoroalkyl substances (PFAS) in municipal and industrial wastewater treatment plants. Water Science & Technology 2021, 84, 3442-3468.
30. Venkatesan, A.K.; Lee, C.S.; Gobler, C.J. Hydroxyl-radical based advanced oxidation processes can increase perfluoroalkyl substances beyond drinking water standards: Results from a pilot study. Science of the Total Environment 2022, 847, 157577.
31. Alalm, M.G.; Boffito, D.C.; Mechanisms and pathways of PFAS degradation by advanced oxidation and reduction processes: A critical review. Chemical Engineering Journal 2022, 450, 138352.
32. Ambaye, T.G.; Vaccari, M.; Prasad, S.; Rtimi, S. Recent progress and challenges on the removal of per- and poly-fluoroalkyl substances (PFAS) from contaminated soil and water. Environmental Science and Pollution Research 2022, 29, 58405–58428.
33. Eun, H.; Shimamura, K.; Asano, T.; Yamazaki, E.; Taniyasu, S.; Yamashita, N. Removal of perfluoroalkyl substances from water by activated carbons: Adsorption of perfluorooctane sulfonate and perfluorooctanoic acid. Environmental Monitoring and Contaminants Research 2022, 2, 88–93.
34. Riegel, M.; Haist-Gulde, B.; Sacher, F. Sorptive removal of short-chain perfluoroalkyl substances (PFAS) during drinking water treatment using activated carbon and anion exchanger. Environmental Sciences Europe 2023, 35, 1-12
35. Zango, Z.U.; Khoo, K.S.; Garba, A.; Kadir, H.A.; Usman, F.; Zango, M.U.; Oh, W.D.; Lim, J.W. A review on superior advanced oxidation and photocatalytic degradation techniques for perfluorooctanoic acid (PFOA) elimination from wastewater. Environmental Research 2023, 221, 115326.
36. Vellanki1, B.P.; Batchelor, B.; Abdel-Wahab, A. Advanced Reduction Processes: A New Class of Treatment Processes. Environmental Engineering Science 2013, 30, 264-271.
37. Gu, Y.; Liu, T.; Zhang, Q.; Dong, W. Efficient decomposition of perfluorooctanoic acid by a high photon flux UV/sulfite process: Kinetics and associated toxicity. Chemical Engineering Journal 2017, 326, 1125–1133.
38. Ren, Z.; Bergmann, U.; Leiviska, T. Reductive degradation of perfluorooctanoic acid in complex water matrices by using the UV/sulfite process. Water Research 2021, 205, 117676.
39. Jian-hua Cheng, J.H.; Liang, X.Y.; She-wei Yang, S.W.; Hu, Y.Y. Photochemical defluorination of aqueous perfluorooctanoic acid (PFOA) by VUV/Fe^{3+} system. Chemical Engineering Journal 2014, 239, 242–249.
40. Gu, Y.; Liu, T.; Wang, H.; Han, H.; Dong, W. Hydrated electron based decomposition of perfluorooctane sulfonate (PFOS) in the VUV/sulfite system. Science of the Total Environment 2017, 607–608, 541–548.
41. Cardoso, I.M.F.; Cardoso, R.M.F.; Esteves da Silva, J.C.G. Advanced Oxidation Processes Coupled with Nanomaterials for Water Treatment. Nanomaterials 2021, 11, 2045.
42. Cardoso, R.M.F.; Cardoso, I.M.F.; da Silva, L.P.; Esteves da Silva, J.C.G. Copper(II)-Doped Carbon Dots as Catalyst for Ozone Degradation of Textile Dyes. Nanomaterials 2022, 12, 1211.
43. Cardoso, I.M.F.; Cardoso, R.M.F.; Pinto da Silva, L.; Esteves da Silva, J.C.G. UV-Based Advanced Oxidation Processes of Remazol Brilliant Blue R Dye Catalyzed by Carbon Dots. Nanomaterials 2022, 12, 2116.
44. Lin, A.Y.C.; Panchangam, S.C.; Chang, C.Y.; P.K. Hong, P.K.A.; Hsueh, H.F. Removal of perfluorooctanoic acid and perfluorooctane sulfonate via ozonation under alkaline condition. Journal of Hazardous Materials 2012, 243, 272– 277.

45. Schroder, H.F.; Meesters, R.J.W. Stability of fluorinated surfactants in advanced oxidation processes— A follow up of degradation products using flow injection–mass spectrometry, liquid chromatography–mass spectrometry and liquid chromatography–multiple stage mass spectrometry. Journal of Chromatography A, 2005, 1082, 110–119.
46. Franke, V.; Schäfers, M.D.; Lindberg, J.J.; Ahrens, L. Removal of per- and polyfluoroalkyl substances (PFASs) from tap water using heterogeneously catalyzed ozonation. Environ. Sci.: Water Res. Technol. 2019, 5, 1887-1896.
47. Dai, X.; Xie, Z.; Dorian, B.; Gray, S.; Zhang, J. Comparative study of PFAS treatment by UV, UV/ozone, and fractionations with air and ozonated air. Environ. Sci.: Water Res. Technol. 2019, 5, 1897-1907.
48. Merényi, G.; Lind, J.; Naumov, S.; Sonntag, C.V. Reaction of Ozone with Hydrogen Peroxide (Peroxone Process): A Revision of Current Mechanistic Concepts Based on Thermokinetic and Quantum-Chemical Considerations. Environ. Sci. Technol. 2010, 44, 3505–3507.
49. Rekhate, C.V.; Srivastava, J.K. Recent advances in ozone-based advanced oxidation processes for treatment of wastewater- A review. Chemical Engineering Journal Advances 2020, 3, 100031.
50. Sauleda, R.; Brillas, E. Mineralization of aniline and 4-chlorophenol in acidic solution by ozonation catalyzed with Fe^{2+} and UVA light. Applied Catalysis B: Environmental 2001, 29, 135–145.
51. Vatankhah, H.; Bahareh Tajdini, B.; Milstead, R.P.; Clevenger, E.; Murray, C.; Knappe, D.; Remucal, C.K.; Bellona, C. Impact of ozone-biologically active filtration on the breakthrough of Perfluoroalkyl acids during granular activated carbon treatment of municipal wastewater effluent. Water Research 2022, 223, 118988.
52. Javed, H.; Lyu, C.; Sun, R.; Zhang, D.; Alvarez, P.J.J. Discerning the inefficacy of hydroxyl radicals during perfluorooctanoic acid degradation. Chemosphere 2020, 247, 125883.
53. Giria, R.R.; Ozaki, H.; Okada, T.; Taniguchi, S.; Takanami, R. Factors influencing UV photodecomposition of perfluorooctanoic acid in water. Chemical Engineering Journal 2012, 180, 197–203.
54. Umar, M. Reductive and Oxidative UV Degradation of PFAS—Status, Needs and Future Perspectives. Water 2021, 13, 3185.
55. Leonello, D.; Fendrich, M.A.; Parrino, F.; Patel, N.; Orlandi, M.; Miotello, A. Light-Induced Advanced Oxidation Processes as PFAS Remediation Methods: A Review. Appl. Sci. 2021, 11, 8458.
56. Hori, H.; Hayakawa, E.; Einaga, H.; Kutsuna, S.; Koike, K.; Ibusuki, T.; Kiatagawa, H.; Arakawa, R. Decomposition of Environmentally Persistent Perfluorooctanoic Acid in Water by Photochemical Approaches. Environ. Sci. Technol. 2004, 38, 6118–6124.
57. Hori, H.; Yamamoto, A.; Hayakawa, E.; Taniyasu, S.; Yamashita, N.; Kutsuna, S.; Kiatagawa, H.; Arakawa, R. Efficient Decomposition of Environmentally Persistent Perfluorocarboxylic Acids by Use of Persulfate as a Photochemical Oxidant. Environ. Sci. Technol. 2005, 39, 2383–2388.
58. Hori, H.; Murayama, M.; Inoue, N.; Ishida, K.; Kutsuna, S. Efficient mineralization of hydroperfluorocarboxylic acids with persulfate in hot water. Catalysis Today 2010, 151, 131–136.
59. Liu, C.S.; Higgins, C.P.; Wang, F.; Shih, K. Effect of temperature on oxidative transformation of perfluorooctanoic acid (PFOA) by persulfate activation in water. Separation and Purification Technology 2012, 91, 46–51.
60. Yang, S.; Cheng, J.; Sun, J.; Hu, Y.; Liang, X. Defluorination of Aqueous Perfluorooctanesulfonate by Activated Persulfate Oxidation. PLOS ONE 2013, 8, e74877.
61. Park, S.; Lee, L.S.; Medina, V.F.; Zull, A.; Waisner, S. Heat-activated persulfate oxidation of PFOA, 6:2 fluorotelomer sulfonate, and PFOS under conditions suitable for in-situ groundwater remediation. Chemosphere 2016, 145, 376-383.
62. Gatto, S.; Sansotera, M.; Persico, F.; Gola, M.; Pirola, C.; Panzeri, W.; Navarrini, W.; Bianchi, C.L. Surface fluorination on TiO2 catalyst induced by photodegradation of perfluorooctanoic acid. Catalysis Today 2015, 241, 8–14.
63. Chen, M.J.; Lo, S.L.; Lee, Y.C.; Huang, C.C. Photocatalytic decomposition of perfluorooctanoic acid by transition-metal modified titanium dioxide. Journal of Hazardous Materials 2015, 288, 168–175.
64. Li, F.; Wei, Z.; He, K.; Blaney, L.; Cheng, X.; Xu, T.; Liud, W.; Zhao. D. A concentrate-and-destroy technique for degradation of perfluorooctanoic acid in water using a new adsorptive photocatalyst. Water Research 2020, 185, 116219.
65. Wang, J.; Cao, C.; Wang, Y.; Wang, Y.; Sun, B.; Zhu, L. In situ preparation of *p-n* BiOI@Bi_5O_7I heterojunction for enhanced PFOA photocatalytic degradation under simulated solar light irradiation. Chemical Engineering Journal 2020, 391, 123530.
66. Yang, Y.; Ji, W.; Li, X.; Zheng, Z.; Bi, F.; Yang, M.; Xu, J.; Zhang, X. Insights into the degradation mechanism of perfluorooctanoic acid under visible-light irradiation through fabricating flower-shaped Bi_5O_7I/ZnO *n-n* heterojunction microspheres. Chemical Engineering Journal 2021, 420, 129934.
67. Kurian, M. Advanced oxidation processes and nanomaterials -a review. Cleaner Engineering and Technology 2021, 2, 100090.
68. Arora, B.; Attri, P. Carbon Nanotubes (CNTs): A Potential Nanomaterial for Water Purification. J. Compos. Sci. 2020, 4, 135.
69. Steven J. Chow, S.J.; Croll, H.C.; Ojeda, N.; Klamerus, J.; Capelle, R.; Oppenheimer, J.; Jacangelo, J.G.; Schwab, K.J; Prasse, C. Comparative investigation of PFAS adsorption onto activated carbon and anion exchange resins during long-term operation of a pilot treatment plant. Water Research 2022, 226, 119198.
70. Das, R.; Leo, B.F.; Murphy, F. The Toxic Truth About Carbon Nanotubes in Water Purification: a Perspective View. Nanoscale Research Letters 2018, 13, 183.
71. Esteves da Silva, J.C.G.; Gonçalves, H. Analytical and bioanalytical applications of carbon dots. TrAC - Trends in Analytical Chemistry 2011, 30, 1327-1336.
72. Meng, W.; Bai, X.; Wang, B.; Liu, Z.; Lu, S.; Yang. B. Biomass-Derived Carbon Dots and Their Applications. Energy & Environmental Materials 2019, 2, 172–192.

73. Li, J.; Xiaohan Li, X.; Da, Y.; Yu, J.; Long, B.; Zhang, P.; Bakker, C.; McCarl, B.A.; Yuan, J.S.; Dai, S.D. Sustainable environmental remediation via biomimetic multifunctional lignocellulosic nano-framework. Nature Communications 2022, 13, 4368.
74. Silva, A.R.; Duarte, M.S.; Alves, M.M.; Pereira, L. Bioremediation of Perfluoroalkyl Substances (PFAS) by Anaerobic Digestion: Effect of PFAS on Different Trophic Groups and Methane Production Accelerated by Carbon Materials. Molecules 2022, 27, 1895.
75. Douna, B.K.; Yousefi, H. Removal of PFAS by Biological Methods. Asian Pac Environ Cancer 2023, 6, 53-64.
76. Smith, S.J.; Wiberg, K.; McCleaf, P.; Ahrens, L. Pilot-Scale Continuous Foam Fractionation for the Removal of Per- and Polyfluoroalkyl Substances (PFAS) from Landfill Leachate. ACS EST Water 2022, 2, 841−851.
77. Wang, Y.; Ji, Y.; Tishchenko, V.; Huang, Q. Removing per- and polyfluoroalkyl substances (PFAS) in water by foam fractionation. Chemosphere 2023, 311, 137004.
78. Morrison, A.L.; Strezov, V.; Niven, R.K.; Taylor, M.P.; Wilson, S.P.; Wang, J.; Burns, D.J.; Murphy, P.J.C. Impact of Salinity and Temperature on Removal of PFAS Species from Water by Aeration in the Absence of Additional Surfactants: A Novel Application of Green Chemistry Using Adsorptive Bubble Fractionation. Ind. Eng. Chem. Res. 2023, 62, 5635−5645.
79. Jia, L.; Liu, W.; Cao, J.; Wu, Z.; Yang, C. Recovery of nanoparticles from wastewater by foam fractionation: Regulating bubble size distribution for strengthening foam drainage. Journal of Environmental Chemical Engineering 2021, 9, 105383.
80. Lei, X.; Lian, Q.; Zhang, X.; Karsili, T.K.; Holmes, W.; Chen, Y.; Zappi, M.E.; Gang, D.D. A review of PFAS adsorption from aqueous solutions: Current approaches, engineering applications, challenges, and opportunities. Environmental Pollution 2023, 321, 121138.
81. Yin, S.; López, J.F.; Solís, J.J.C.; Wong, M.S.; Villagrán, D. Enhanced adsorption of PFOA with nano MgAl2O4@CNTs: influence of pH and dosage, and environmental conditions. Journal of Hazardous Materials Advances 2023, 9, 2023, 100252.
82. Karbassiyazdi, E.; Medha Kasula, M.; Sweta Modak, S.; Pala, J.; Kalantari, M.; Altaee, A.; Esfahani, M.R.; Razmjou, A. A juxtaposed review on adsorptive removal of PFAS by metal-organic frameworks (MOFs) with carbon-based materials, ion exchange resins, and polymer adsorbents. Chemosphere 2023, 311, 136933.
83. Wen, Y.; Gómez, A.R.; Day, G.S.; Smith, M.F.; Yan, T.H.; Ozdemir, R.O.K.; Gutierrez, O.; Sharma, V.K.; Ma, X.; Zhou, H.C. Integrated Photocatalytic Reduction and Oxidation of Perfluorooctanoic Acid by Metal−Organic Frameworks: Key Insights into the Degradation Mechanisms. J. Am. Chem. Soc. 2022, 144, 11840−11850.
84. Chen, C.; Ma, Q.; Liu, F.; Gao, J.; Li, X.; Sun, S.; Hong Yao, H.; Liu, C.; Young, J.; Zhan, W. Photocatalytically reductive defluorination of perfluorooctanoic acid (PFOA) using Pt/La2Ti2O7 nanoplates: Experimental and DFT assessment. Journal of Hazardous Materials 2021, 419, 126452.
85. Wang , J.; Cao, C.; Zhang, Y.; Zhang Y.; Zhu, L. Underneath mechanisms into the super effective degradation of PFOA by BiOF nanosheets with tunable oxygen vacancies on exposed (101) facets. Applied Catalysis B: Environmental 2021, 286, 119911.
86. Ji, H.; Ni, J.; Zhao, D.; Liu, W. Application of Titanate Nanotubes for Photocatalytic Decontamination in Water: Challenges and Prospects. ACS EST Engg. 2022, 2, 1015−1038.
87. Zhu, Y.; Xu, T.; Zhao, D.; Li, F.; Liu, W.; Wang, B.; An, B. Adsorption and solid-phase photocatalytic degradation of perfluorooctane sulfonate in water using gallium-doped carbon-modified titanate nanotubes. Chemical Engineering Journal 2021, 421, 129676.
88. Zhu, Y.; Xu, T.; Zhao, D. Metal-doped carbon-supported/modified titanate nanotubes for perfluorooctane sulfonate degradation in water: Effects of preparation conditions, mechanisms, and parameter optimization. Science of the Total Environment 2022, 853, 158573.
89. Zhu, Y.; Ji, H.; He, K.; Blaney, L.; Xu, T.; Zhao, D. Photocatalytic degradation of GenX in water using a new adsorptive photocatalyst. Water Research 2022, 220, 118650.
90. Kundu, S.; Radian, A. Surface confinement of per-fluoroalkyl substances on an iron-decorated clay-cyclodextrin composite enables rapid oxidation by hydroxyl radicals. Chemical Engineering Journal 2022, 431, 134187.
91. Duan, L.; Wang, B.; Kimberly Heck, N.; Clark, C.A.; Wei, J.; Wang, M.; Metz, J.; Wu, G.; Tsai, A.L.T.; Guo, S.; Arredondo, J.; Mohitec, A.D.; Senftle, T.P.; Westerho, P.; Alvarez, P.; Wen, J.A.; Song, Y.; Wong, M.S. Titanium oxide improves boron nitride photocatalytic degradation of perfluorooctanoic acid. Chemical Engineering Journal 2022, 448, 137735.
92. Schlesinger, D.R.; McDermott, C.; Le, N.Q.; Ko, J.S.; Johnson, J.K.; Demirev, P.A.; Xia, Z. Destruction of per/poly-fluorinated alkyl substances by magnetite nanoparticle-catalyzed UV-Fenton reaction. Environ. Sci.: Water Res. Technol., 2022, 8, 2732.
93. Metz, J.; Zuo, P.; Wang, B.; Wong, M.S.; Alvarez, P.J.J. Perfluorooctanoic acid Degradation by UV/Chlorine. Environ. Sci. Technol. Lett. 2022, 9, 673−679.
94. Trang, B.; Li□, Y.; Xue, X.S.; Ateia, M.; Houk, K.N.; Dichtel. W.R. Low-temperature mineralization of perfluorocarboxylic acids. Science 2022, 377, 839.